Cellulose (2024) 31:6373–6385
https://doi.org/10.1007/s10570-024-05972-z

ORIGINAL RESEARCH

Dynamic Schiff base linkage-based double-network hydrogels with injectable, self-healing, and pH-responsive properties for bacteria-infected wound healing

Wenfang Du · Hong Li · Jie Luo · Yuxiao Wang · Qiang Xi · Jie Liu · Shengyuan Yang · Junjie Li · Fubing Xiao

Received: 17 September 2023 / Accepted: 21 May 2024 / Published online: 30 May 2024

Abstract The development of wound dressing materials with both self-healing and antibacterial properties for promoting wound closure is highly desirable in health care. Herein, a smart double-network hydrogel (GS/DPPDH) with promising traits was developed by combining a dynamic Schiff base reaction between dialdehyde carboxymethyl cellulose (DCMC) and poly(ethylene imine) (PEI) with free radical polymerization. Because of its abundant amino groups, the common antibacterial drug gentamycin sulfate (GS) can be loaded into hydrogels by the formation of Schiff base bonds with DCMC. The slightly acidic wound microenvironment caused hydrolysis of the Schiff base bonds, thus releasing the drug GS on-demand. The prepared hydrogel not only showed good self-healing and injectable properties but also displayed excellent blood compatibility and cytocompatibility. The in vitro antibacterial experimental data proved that the GS/DPPDH had high antibacterial ratios of nearly 90% against both gram-positive (*S. aureus*) and gram-negative (*E. coli*) bacteria. In addition, in vivo assessment in a mouse model of *S. aureus*-infected full-thickness skin wounds revealed a wound closure ratio of 83.22 ± 2.90% after 7 days of healing, which was significantly greater than that in the gauze (59.78 ± 2.60%) and DPPDH (66.08 ± 0.21%) groups. Taken together, the results showed that the prepared antibacterial double-network hydrogel with injectable, self-healing, and pH-responsive properties exhibits great potential as a dressing material for infected wound healing.

Wenfang Du and Hong Li contributed equally to this work.

Supplementary Information The online version contains supplementary material available at https://doi.org/10.1007/s10570-024-05972-z.

W. Du · H. Li · J. Luo · Y. Wang · J. Liu · S. Yang · F. Xiao (✉)
Hunan Key Laboratory of Typical Environmental Pollution and Health Hazards, School of Public Health, Hengyang Medical School, University of South China, Hengyang 421001, China
e-mail: xiaofubing2008@163.com

W. Du · Q. Xi · J. Li (✉) · F. Xiao
State Key Laboratory of Chemo/Biosensing and Chemometrics, College of Chemistry and Chemical Engineering, Hunan University, Changsha 410082, China
e-mail: junjieli9007@163.com

W. Du
College of Biological and Environmental Engineering, Binzhou University, Binzhou 256600, China

Q. Xi
Hunan Prevention and Treatment Institute for Occupational Diseases, Affiliated Prevention and Treatment Institute for Occupational Diseases of University of South China, Changsha 410007, China

Keywords Dialdehyde carboxymethyl cellulose · Double-network hydrogel · Self-healing · On-demand drug release · Infected wound healing

Introduction

The skin is the largest organ of the body and covers its entire surface, acting as a physical/chemical barrier to protect the internal organs from external damage and microbial invasion (Dong et al. 2022; Du et al. 2022; Qu et al. 2022; Sun et al. 2023; Yang et al. 2023). Owing to its direct contact with the external environment, the skin is also highly susceptible to injury and infection (Qiao et al. 2023). Once the skin suffers severe collapse, the resulting wound can affect the health of the patient and may even endanger the patient's life (Li et al. 2022; Zou et al. 2022). Wound repair is a complex process that includes four phases: bleeding cessation, inflammation, proliferation, and remodelling (Qian et al. 2022). To promote wound closure, many new dressing materials, such as foams (Patil et al. 2022; Xie et al. 2022), electrospun scaffolds (Chen et al. 2021; Yue et al. 2021), films (Alzarea et al. 2022; Zhang et al. 2021; Zhao et al. 2022), and hydrogels (Cao et al. 2023; Cui et al. 2023; Ding et al. 2021; Dong et al. 2023; Sun et al. 2021; Zhao et al. 2020), have been proposed. Among these materials, hydrogels, as a new kind of functional material (Tang et al. 2023; Xiao et al. 2016, 2017), are widely used in the fields of biomedicine and analysis (Du et al. 2023; Xiao et al. 2022; Zhu et al. 2023) and are considered the most promising wound dressing owing to their good hydrophilicity, air permeability, and biocompatibility (Guo et al. 2023; Li and Mooney 2016; Zhang and Khademhosseini 2017). In particular, self-healing hydrogels that can be injected and form in situ, fit wounds of different shapes, and encapsulate drugs, can accelerate wound repair via multiple processes.

Cellulose-based self-healing hydrogels generated via Schiff base reactions have attracted widespread interest due to their good self-healing ability and excellent biocompatibility (Mallakpour et al. 2021; Wang et al. 2023). Cellulose is a renewable, biodegradable, and green material that is widely present in the cell walls of plant biomass (Sharma et al. 2021; Shen et al. 2021). Carboxymethyl cellulose (CMC), an important cellulose derivative, contains abundant o-hydroxyl groups that can be oxidized by periodate to generate dialdehyde CMC (DCMC) (Wang et al. 2019). The very large number of aldehyde groups in DCMC can interact with amino group-containing polymers in a Schiff base reaction to generate a self-healing hydrogel. Chang developed a self-healing hydrogel based on carboxymethyl chitosan and CMC, which was used to promote diabetic wound healing (Chang et al. 2022). In addition, Zou proposed a multifunctional bio-adhesive hydrogel utilizing dynamic covalent bonds, light-triggered covalent bonds, and hydrogen bonds (Zou et al. 2022). However, Schiff base hydrogels usually suffer from poor toughness, which may limit their application. We therefore anticipate constructing a double-network hydrogel by introducing another polymer to enhance the mechanical strength of the hydrogel dressing.

To prevent wound infection, antibacterial agents are usually incorporated into wound dressings to inhibit microbial metabolism. However, overuse or abuse of antibiotics may promote bacterial evolution, giving rise to drug-resistant microorganisms (Ran et al. 2022; Tang et al. 2022a, 2022b; Zhou et al. 2023). Therefore, on-demand drug release is essential for hydrogel wound dressings to accelerate skin wound closure. Bacterial growth and metabolism at wound sites are known to produce organic acids such as lactic acid and acetic acid, resulting in local acidification (Hu et al. 2021; Liu et al. 2022; Weinstein 1985). Accordingly, the development of a pH-responsive self-healing hydrogel that regulates drug release through changes in wound pH represents an ideal way to minimize side effects. Schiff bases are hydrolyzed in mildly acidic environments (Liang et al. 2022). Motivated by this, we reason that a drug could be encapsulated in a hydrogel via Schiff base bonds for pH-responsive drug release.

Herein, we aimed to develop a smart double-network hydrogel with injectable, self-healing, and pH-responsive characteristics for antibacterial wound healing based on dynamic Schiff base reactions and free radical reactions (Scheme 1). The hydrogel was fabricated by using UV photopolymerization of a mixture of poly(ethylene glycol) diacrylate (PEGDA), DCMC, poly(ethylene imine) (PEI), 2-hydroxy-2-methylpropiophenone (HMPP), and gentamycin sulfate (GS). The first network was formed by creating reversible Schiff base bonds between aldehyde-modified DCMC and amine-containing PEI, which endowed the hydrogel

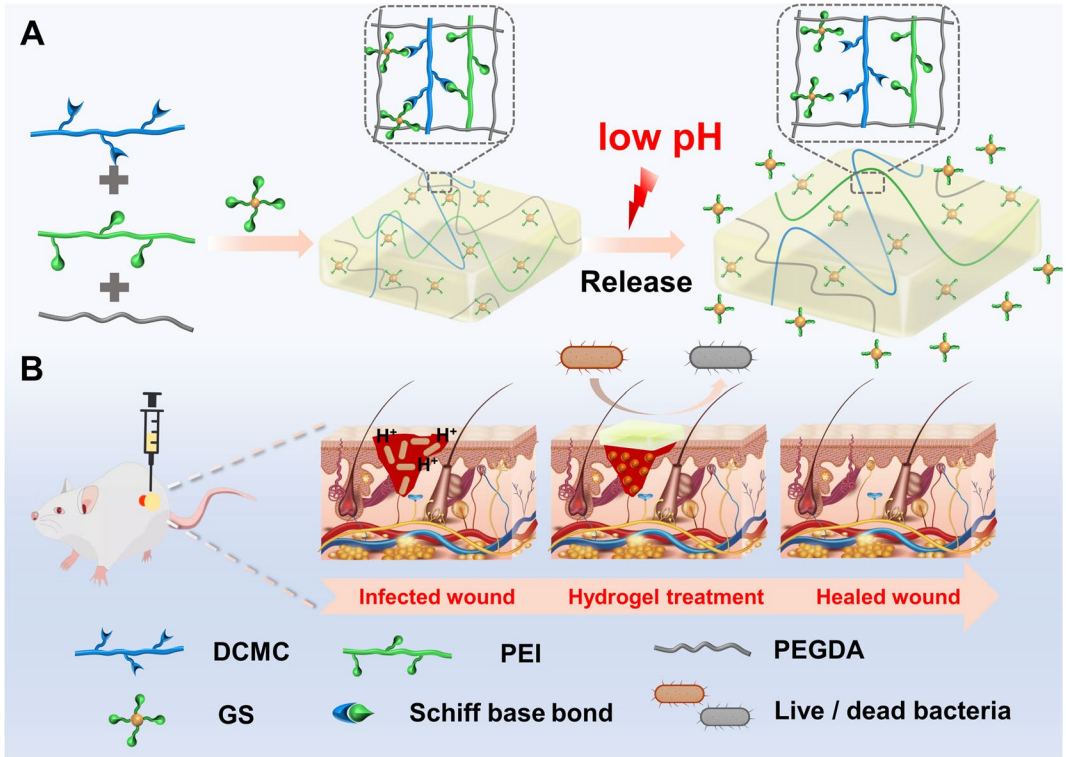

Scheme 1. (A) Synthetic route of the double-network hydrogel. (B) The double-network hydrogel kills bacteria by releasing antibiotics and accelerates wound healing

with injectability and self-healing abilities. To increase the mechanical strength of the hydrogel, the second network was introduced via the free radical photopolymerization of PEGDA by using HMPP as the photoinitiator. Moreover, the antibacterial drug GS was reversibly bonded to the hydrogel network by a Schiff base linkage between the aldehyde in DCMC and the amino group in GS. In acidic bacteria-infected wounds, dynamic Schiff base bonds are hydrolyzed upon hydrogel disintegration, releasing GS. The released GS can kill bacteria rapidly, thereby reducing bacterial infection. This work provides a novel injectable and self-healing double-network hydrogel with excellent mechanical properties and realizes on-demand antibacterial drug release to promote wound repair via multiple processes.

Experimental section

Reagents and materials

Sodium carboxymethyl cellulose (CMC, viscosity 800–1200 mPa·s, USP grade; the structure is shown in Fig. S1), sodium periodate ($NaIO_4$), PEGDA (average molecular weight of 600 g/mol), HMPP, GS, and PEI (average molecular weight of 10,000 g/mol, 99%) were purchased from Aladdin Reagent Co., Ltd (Shanghai, China). Male Sprague–Dawley mice (12 weeks old, 200–240 g) were obtained from Hunan SJA Laboratory Animal Co., Ltd. All mice were fed and tested in accordance with the Department of Laboratory Animal Science at the

University of South China rules and guidelines. *E. coli* (ATCC 25922) and *S. aureus* (ATCC 29213) were obtained from the China General Microbiological Culture Collection Centre.

Preparation of the hydrogels

The prepolymer solution was a mixture of PEI (1.16%, v/v), DCMC (6.50%, w/v), PEGDA (6.00%, v/v), and HMPP (0.60%, v/v). The liquid prepolymer was irradiated with 365 nm UV light to form a DCMC-PEI/PEGDA double-network hydrogel (DPPDH). To encapsulate GS in the hydrogel, GS solution (150 mg/mL) mixed with the DCMC solution and allowed to react for 30 min at 37 °C, after which the GS drug-loaded DPPDH (GS/DPPDH) was prepared via the same method as that used for the DPPDH.

Self-healing, injectable, and mechanical properties

In the macroscopic self-healing experiment, a heart-shaped hydrogel was cut in half with a scalpel, and one piece was dyed with methylene blue. Then, the two pieces were put back together, and the self-healing process was observed and photographed. The tests were repeated three times (n = 3). To assess the injectability of the hydrogels, the hydrogels were loaded into a 1 mL syringe and extruded through needles to produce specific shapes and letters. Hydrogel samples with cylindrical shapes were prepared (6 mm in both diameter and thickness) and pressed with fingers to test their compression properties.

Release of GS from the hydrogels in vitro

GS/DPPDH (5 cm × 1.5 cm × 0.5 mm, n = 3) were immersed in 20 mL of phosphate-buffered saline (PBS; pH 6.0, 7.4, or 8.0) at 37 °C. At different time points, 0.4 mL of the solution was removed for UV−Vis detection by using a UV−Vis spectrophotometer (UV-2550, Shimadzu). After each measurement, 0.4 mL of PBS solution was added back to the system. The concentration of the released GS was determined by using a standard curve.

Hemolysis test of the hydrogels

Hydrogel disc samples (6 mm diameter, n = 3) were soaked in 1.5 mL of red blood cells in PBS. After incubation at 37 °C for 1 h, the dispersion was centrifuged at 1500 rpm for 10 min. The absorbance values were subsequently measured at 545 nm by utilizing a microporous plate detecting instrument (Cytation 3, 1,606,239). The hemolysis ratio (%) was calculated as $(A_{sample} - A_{negative})/(A_{positive} - A_{negative}) \times 100\%$ (n = 3), where A_{sample}, $A_{positive}$, and $A_{negative}$ are the absorbance values of the sample, the positive control, and the negative control, respectively.

Antibacterial properties of the hydrogels

The modified disk diffusion method was performed as follows. Briefly, 0.1 mL of bacterial solution (10^6–10^7 CFU/mL) was seeded evenly onto a Luria–Bertani (LB) agar plate with a swab. Then, the cylinder-shaped hydrogels (6 mm in diameter) were placed on the surface of the LB agar plate after being sterilized under ultraviolet light. After incubating at 37 °C for 24 h, images of the plates were taken, and the diameter of the inhibition zone was measured by using an electronic digital caliper.

To further study the antibacterial activity of the hydrogels, bacterial growth curves were constructed, and agar plate counting experiments were carried out. Briefly, *E. coli* and *S. aureus* suspensions (10^5 CFU/mL, 20 mL) were added to small glass bottles containing hydrogels (20 mm × 10 mm × 0.5 mm). During incubation, the changes in turbidity of the bacterial solutions were observed, and the OD600 values were measured at specific points in time. After incubation for 24 h, 15 μL of bacterial solution was uniformly inoculated on an agar plate. After incubation at 37 °C for 24 h, the plates were photographed. The antibacterial ratio (%) was calculated as $(OD_{control} - OD_{sample})/OD_{control} \times 100\%$ (n = 3), where $OD_{control}$ and OD_{sample} are the OD600 values of the control group and experimental group, respectively.

In vivo wound healing assay

Mice were randomly divided into 3 groups (6 mice per group) after being acclimatized for 3 days. Subsequently, the mice were anesthetized by injection of 10% chloral hydrate, and the right back area of

the mice was shaved off with a razor. After that, 1 cm diameter full-thickness skin wounds were created. Then, the wounds were infected with 20 µL of *S. aureus* (10^8 CFU/mL). After surgery, the wounds were covered with gauze, DPPDH, or GS/DPPDH depending on the group. The wound area was photographed and analyzed by drawing and measuring the wound boundaries using ImageJ software. The wound closure ratio (%) was calculated as $(S_{0\ day} - S_{n\ day})/S_{0\ day} \times 100\%$ (n = 3), where $S_{0\ day}$ and $S_{n\ day}$ are the wound areas on Day 0 and Day n, respectively.

For biochemical analysis, wound tissue samples were collected on Days 5 and 10.

Results and discussion

Preparation and characterization of the hydrogels

The double-network hydrogel was constructed via a Schiff base reaction and free radical polymerization (Scheme 1). First, CMC was oxidized by sodium periodate to produce DCMC, which possesses abundant dialdehyde groups (Fig. S1). The structure of DCMC was verified by using ATR-FTIR spectroscopy (Fig. 1A). After comparison to the CMC spectrum, the characteristic absorption peak of DCMC appeared at 1740 cm^{-1} in the product spectrum, which is the stretching vibration of the free aldehyde group. The aldehyde content of DCMC was calculated to be 40% according to Equation (S1). The above data

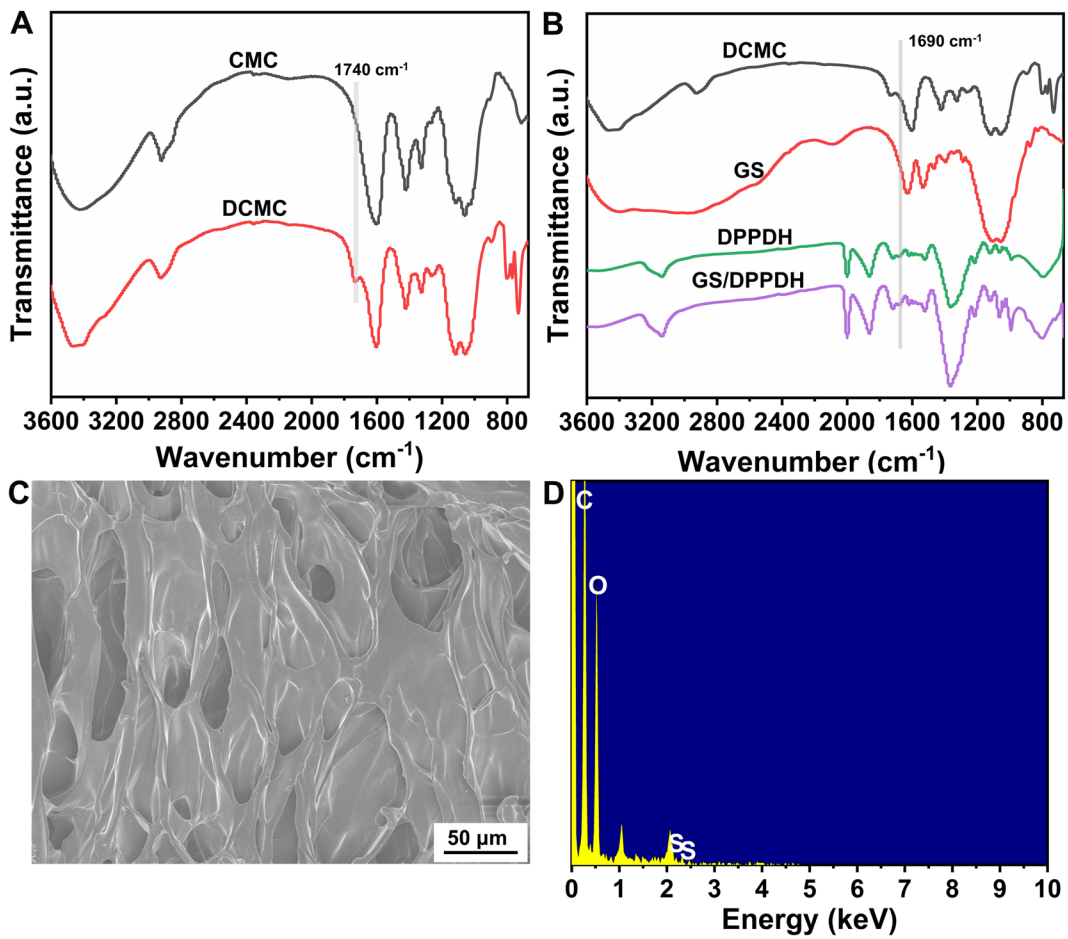

Fig. 1 (**A**) ATR-FTIR spectra of CMC and DCMC. (**B**) ATR-FTIR spectra of DCMC, GS, DPPDH, and GS/DPPDH. (**C**) SEM image of GS/DPPDH. (**D**) EDS mappings of GS/DPPDH

suggested that the CMC was successfully transformed into DCMC. Then the hydrogel was cross-linked by the formation of dynamic Schiff base bonds between DCMC and PEI. To adjust the mechanical strength of the hydrogel, PEGDA was introduced as the second cross-linker via a free radical reaction to construct a DCMC-PEI/PEGDA double-network hydrogel (DPPDH). According to Fig. S2, the mechanical strength of the DPPDH was greater than that of the DCMC-PEI hydrogel without PEGDA cross-linking. According to Fig. 1B, a new peak at 1690 cm^{-1} corresponding to the imine bond (C = N) appeared in the spectra of the DPPDH and GS/DPPDH, indicating the formation of Schiff base bonds.

The microstructures of the hydrogels were observed via SEM (Fig. 1C). It was observed that the GS/DPPDH possessed three-dimensional porous structures conducive to nutrient transport, cell adhesion, and proliferation. To further explore whether GS can be loaded into the hydrogel, EDS was performed to explore the interaction between GS and the hydrogel. As shown in Fig. 1D, the GS/DPPDH displayed intense sulfur peaks, confirming that the drug GS was successfully loaded into the hydrogel.

Self-healing, injectable, mechanical, and adhesive behaviors

Self-healing performance is critical for a hydrogel to withstand deformation caused by external mechanical forces after it is applied to the wound. Hence, a macroscopic self-healing experiment was conducted to investigate the self-healing ability of the developed GS/DPPDH. As depicted in Fig. 2A, the heart-shaped hydrogel was bisected, and one of the resulting fragments was stained with methylene blue. Subsequently, the two segments were recombined to facilitate self-healing at room temperature, devoid of external stimuli. Over time, the two hydrogel fragments autonomously mended and adhered, demonstrating the capacity for self-healing, as evidenced by their cohesive response upon being lifted with a pair of tweezers. Additionally, optical microscopy images were captured to evaluate the progression of the hydrogel healing process. Notably, the healing boundary of the hydrogel exhibited a gradual blurring effect, ultimately dissipating entirely following complete healing. Rheological experiments were also conducted to further investigate the self-healing ability of the GS/DPPDH by measuring the storage modulus (G′) and loss modulus (G″) values. As depicted in Fig. 2B, the strain sweep curves showed an intersection between G′ and G″ at a strain of 65%, indicating that the hydrogel network collapsed. When the strain was above the critical strain, the G′ value decreased rapidly and was lower than the corresponding G", implying that the hydrogel was in a liquid state. Afterward, step-strain measurements were made. As shown in Fig. 2C, when a large strain (100%) was applied, the G′ value of the GS/DPPDH decreased from 1690 to 300 Pa and was lower than the G" value, indicating damage to the hydrogel network. At a strain of 1%, the G′ and G″ values returned to their initial values even after five damage cycles, indicating the outstanding self-healing ability of the prepared hydrogel. The self-healing properties of the hydrogel were ascribed to the formation of Schiff base bonds between DCMC and PEI.

The injectability of the hydrogel was assessed with extrusion tests (Fig. 2D, 2E, and 2F). Owing to the dynamic nature and shear-thinning property of the hydrogels, hydrogels extruded from needles can self-assemble and self-heal into integral hydrogels and adapt to heart-shaped molds. Moreover, the hydrogel could be extruded from the syringe to draw the letters USC (University of South China) and a pentagram. All of these results proved that the hydrogel had self-healing and injectable capabilities.

The compressibility of the hydrogel was tested by using the finger pressing method (Fig. S3). When the GS/DPPDH was compressed to half of its original volume, it fully recovered its initial shape and size after the pressure was removed. The adhesive properties of the hydrogels were assessed by adhering GS/DPPDH to various materials. GS/DPPDH exhibited good adhesion to glass, cotton, plastic, metal, paper and wood (Fig. S4). Furthermore, when GS/DPPDH was affixed to crooked knuckles, the hydrogel fit and adhered well to the skin surfaces without any retraction or rupture during bending of the finger at different angles (Fig. S5). These results demonstrated that the GS/DPPDH had excellent mechanical and adhesive properties that met the requirements for practical use as a wound dressing.

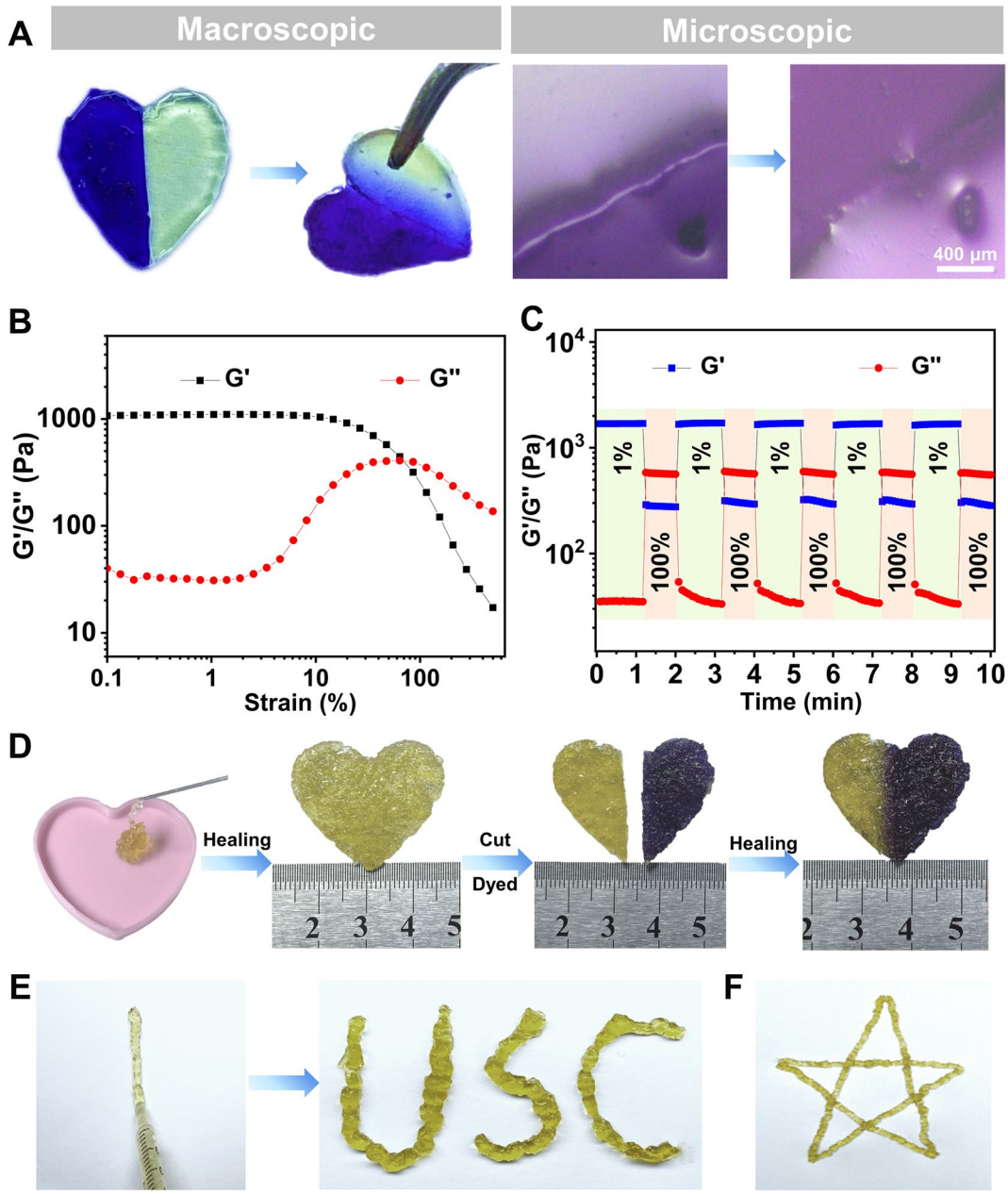

Fig. 2 (**A**) Macroscopic and microscopic self-healing processes of GS/DPPDH. (**B**) Strain sweep tests with GS/DPPDH. (**C**) Step-strain sweep for GS/DPPDH with a strain ranging from 1 to 100%. (**D**, **E**, and **F**) Injectability of GS/DPPDH

Swelling, degradation and GS release behaviors

Hydrogel wound dressings capable of absorbing wound exudates and providing a wet environment are effective for rapid wound repair. Therefore, the swelling behaviors of the hydrogels were investigated by measuring the changes in mass after immersion in PBS at 37 °C (Fig. 3A). The DPPDH and GS/DPPDH swelled rapidly and reached equilibrium within 10 min and 30 min, respectively. The swelling ratios of DPPDH and GS/DPPDH were 323.59% and 310.14%, respectively. The lower swelling ratio of

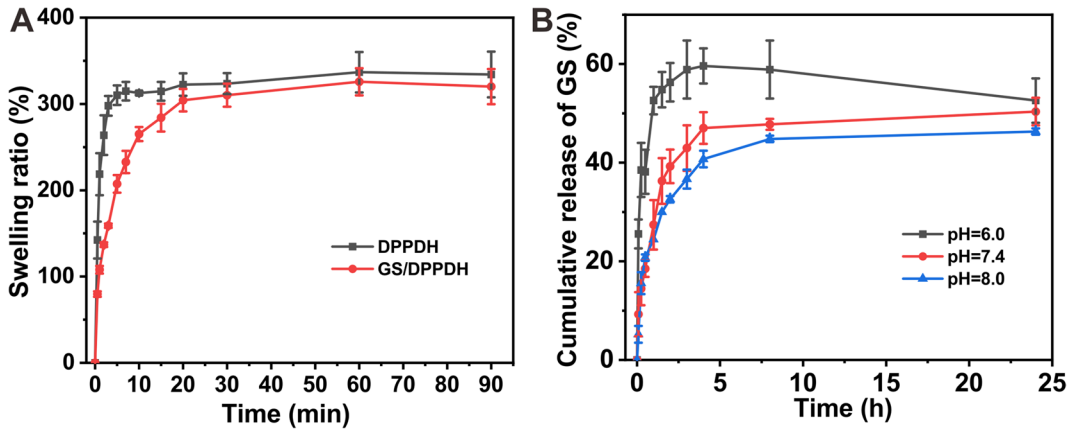

Fig. 3 (**A**) Swelling ratios of the hydrogels in PBS (pH 7.4) at 37 °C (n = 3). (**B**) Release behaviors of GS from GS/DPPDH in PBS at various pH values at 37 °C (n = 3)

the GS/DPPDH was attributed to the addition of GS, which increased the cross-linking density. Hydrogel degradation was also estimated, and the results are shown in Fig. S6. The DPPDH and GS/DPPDH degraded gradually after 24 h and 34 h, respectively, allowing for easy removal of the hydrogel dressing and protection of the wound from damage.

The in vitro release of GS from GS/DPPDH was studied, and the results are illustrated in Fig. 3B. Under physiological conditions (pH 7.4, 37 °C), GS/DPPDH exhibited sustained release of GS, reaching 42% within 4 h before reaching a plateau. Since Schiff base bonds are known to be pH-responsive, the release of GS from the GS/DPPDH at other pH values (6.0 and 8.0) was evaluated. We found that the release rate of GS was relatively fast in an acidic environment (pH 6.0) and release equilibrium was reached after approximately 3 h, but reaching release equilibrium took 8 h in an alkaline environment (pH 8.0). The sensitive pH-induced release of the drug showed that the GS/DPPDH can release antibiotics on-demand according to the pH change in the wound, meeting the actual needs of infected wound healing.

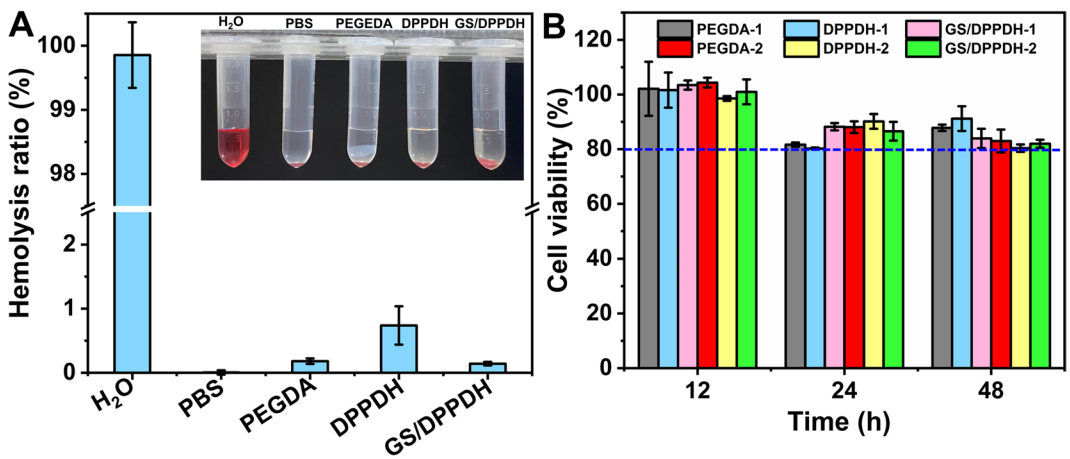

Fig. 4 (**A**) Hemolysis ratios and images of the hydrogels (n = 3). (**B**) Viability of NIH 3T3 cells treated with different concentrations of hydrogel extracts (the concentrations of PEGDA-1, DPPDH-1 and GS/DPPDH-1 were 50 μg/mL; the concentrations of PEGDA-2, DPPDH-2 and GS/DPPDH-2 were 100 μg/mL) (n = 3)

Biocompatibility

The blood compatibility of the hydrogels was assessed through hemolysis assays. As shown in Fig. 4A, neither the negative control (PBS) nor the hydrogel groups exhibited obvious hemolysis, while the positive control group (H_2O) exhibited a noticeable red color. The hemolysis ratios in the PEGDA, DPPDH, and GS/DPPDH groups were 0.13%, 0.56%, and 0.12%, respectively, which are all well below the critical safe range of 5% for biomaterials according to ISO/TR 7406. This suggested the high blood compatibility of the hydrogels. The cellular compatibility of the hydrogels was next studied by assessing the cytotoxicities of the hydrogel extracts by using CCK-8 assays. The mouse embryonic fibroblast cell line NIH 3T3 was cultured in the extracts of different hydrogels (including PEGDA, DPPDH, and GS/DPPDH) for 12, 24, and 48 h. As shown in Fig. 4B, the NIH 3T3 cells in all groups were healthy, and cell viability ranged from 80.20% to 104.30% at the three tested time points. With increasing culture time, cell viability decreased slightly, illustrating that the hydrogels had certain cytotoxicity that was within an acceptable range. All these results indicated that the hydrogels exhibited good biocompatibility and could be used for subsequent infected wound treatment.

In vitro antibacterial properties

An ideal wound dressing with effective antibacterial properties is essential for preventing bacterial infections and promoting wound repair. In the present study, the antibacterial effects of the proposed hydrogel materials against *Escherichia coli* (*E. coli*, gram-negative) and *Staphylococcus aureus* (*S. aureus*, gram-positive) were evaluated via disc diffusion tests. Zones of inhibition against these two microbes were clearly observed in the GS/DPPDH group and were slightly smaller than those in the GS group (Fig. 5A and 5B). This result was attributed to the slow release of GS from GS/DPPDH via hydrolysis of the Schiff base bond. In contrast, no differentiable inhibition zones were formed in the *E. coli* or *S. aureus* DPPDH groups. Additionally, the diameter of the inhibition zone of *S. aureus* was greater than that of *E. coli*, implying that the GS/DPPDH is more effective against gram-positive bacteria.

In addition, contact sterilization experiments were conducted by soaking the hydrogels in *E. coli* and *S. aureus* solutions (10^5 CFU/mL) to further investigate the antibacterial effects of the hydrogels. After 24 h, the culture media of the GS group and GS/DPPDH group were clear and transparent, while those of the DPPDH group and the control group without GS were turbid, demonstrating that the number of bacteria decreased upon the addition of GS/DPPDH (Fig. S7). Moreover, the concentrations of bacteria in the different groups were quantitatively determined by monitoring the optical density at 600 nm (OD600) at different times. As shown in Fig. 5C and 5D, the OD600 values of the two bacteria in the control group and DPPDH group increased gradually with time, suggesting that DPPDH had no antibacterial effects. Conversely, in the presence of either GS or GS/DPPDH, relatively low and constant OD600 values were found throughout the whole testing period, proving that the bacteria were almost completely killed and that GS/DPPDH exhibited stable antibacterial activity. The antibacterial ratios of GS/DPPDH against the two bacteria reached nearly 90% (Fig. 5E and 5F). In addition, a small amount of bacterial solution cultured for 24 h was extracted for colony counting (Fig. 5G). The results showed that almost no colonies grew in the GS or GS/DPPDH groups, while there were large colonies in the DPPDH and control groups. In summary, the above data confirmed that the developed GS/DPPDH exhibited excellent antibacterial activity that was highly important for wound dressing.

In vivo wound healing

Having studied the self-healing and antibacterial capacities of the hydrogels in vitro, our aim was to evaluate the performance of the proposed hydrogels in wound healing in vivo by constructing a mouse model of full-thickness skin defects infected with *S. aureus*. The wounds were treated with gauze (control), DPPDH, or GS/DPPDH for 10 days. As displayed in Fig. 6A and 6B, the wound areas in all three groups progressively decreased. After being treated for 7 days, the wounds in the GS/DPPDH groups were smaller than those in the control and DPPDH groups, indicating that the GS/DPPDH could promote wound closure by inhibiting bacterial growth

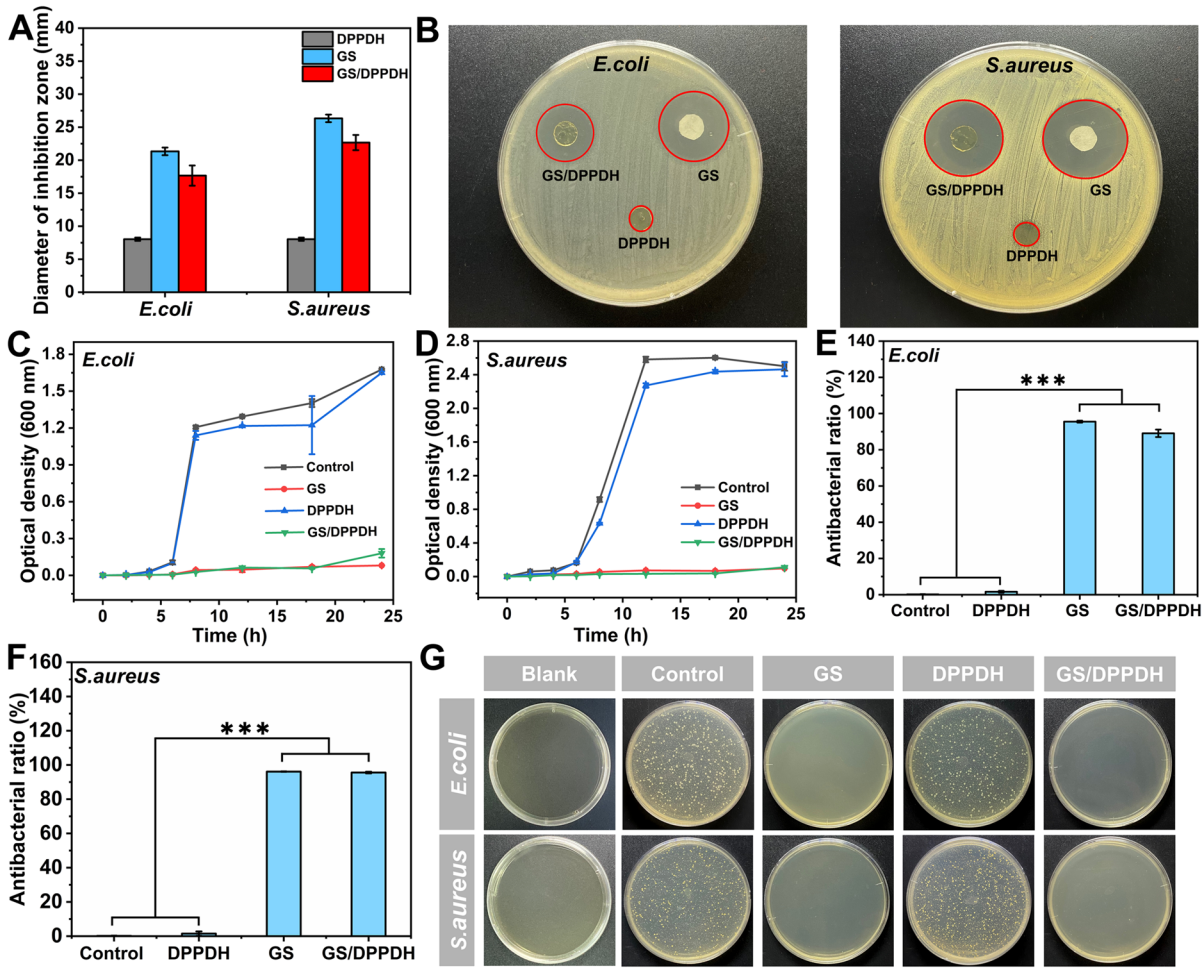

Fig. 5 (**A**) Diameters of the inhibition zones produced by GS, DPPDH, and GS/DPPDH. (**B**) The corresponding photographs of the inhibition zones (n = 3). Growth curves of *E. coli* (**C**) and *S. aureus* (**D**) as a function of culture time in different groups (n = 3). Antibacterial ratios of the different hydrogel samples against *E. coli* (**E**) and *S. aureus* (**F**) at 24 h (n = 3); ***P < 0.001. (**G**) Photographs of the bacterial colonies extracted from the bacterial solutions on agar plates for 24 h (n = 3)

in the wound area. The quantitative wound closure ratios corresponding to the different healing times are shown in Fig. 6C. After 7 days of healing, the wound closure ratios in the gauze, DPPDH, and GS/DPPDH groups reached 59.78 ± 2.60%, 66.08 ± 0.21%, and 83.22 ± 2.90%, respectively. In addition, after 10 days, the wounds in the GS/DPPDH group had almost completely healed, while the wound closure ratios in the DPPDH and gauze groups were still 95.41 ± 0.57% and 94.61 ± 0.81%, respectively. These results indicated that GS/DPPDH was highly effective at accelerating wound healing in vivo.

Hematoxylin and eosin (H&E) staining and Masson's trichrome staining were utilized to investigate wound closure from a histological perspective. As shown in Fig. 6D, after treatment for 5 days, the hydrogel-treated groups had fewer inflammatory cells than the control group did, possibly because these wounds were isolated from outside environment by the hydrogel dressing. The GS/DPPDH group exhibited the sparsest inflammatory response, with more vessels and granulation tissues forming on the wound surface, likely due to the antibacterial activity of the GS released from the GS/DPPDH. Moreover, the

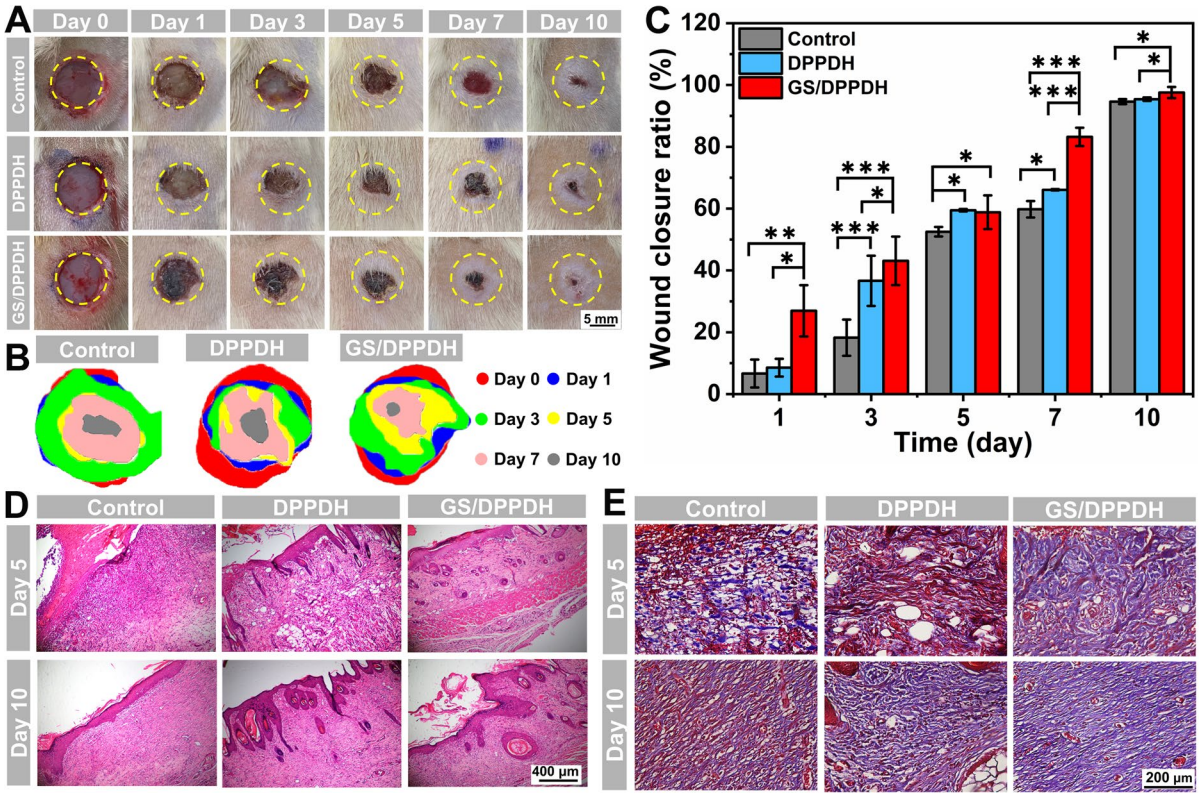

Fig. 6 (**A**) Photographs of the wound areas on Days 0, 1, 3, 5, 7, and 10. (**B**) The corresponding traces of wound closure. (**C**) Wound closure ratios at 10 days (n = 3); *P < 0.05, **P < 0.01, ***P < 0.001. H&E staining (**D**) and Masson's trichrome staining (**E**) images of the skin tissues on Days 5 and 10

collagen levels in the wounds were evaluated by Masson's trichrome staining (Fig. 6E). At the same time point, the GS/DPPDH group exhibited more collagen deposition than the DPPDH and control groups. This was mainly because the GS/DPPDH group maintained an appropriate moist environment and released the antibacterial drug, which are beneficial for wound healing. All these results illustrated that the proposed self-healing hydrogel can serve as an excellent antibacterial wound dressing.

Conclusions

In summary, a novel double-network hydrogel with injectable, self-healing, and pH-responsive capabilities was developed for antibacterial wound healing by using dynamic Schiff base reactions and free radical reactions. The dynamic Schiff base bond between the aldehyde-modified DCMC and amine-containing PEI endowed the hydrogel with injectable and self-healing features. The introduction of a second network structure based on the free radical photopolymerization of PEGDA aimed to regulate the mechanical strength. Furthermore, upon loading the drug GS into the hydrogel via the formation of Schiff base bonds, the proposed hydrogel also exhibited pH-responsiveness for on-demand antibacterial drug release. The hydrogel was proven to have good cytocompatibility and good blood compatibility. The in vivo experimental data demonstrated that this hydrogel dressing had high antibacterial efficacy and accelerated skin wound healing in mice. Collagen deposition also increased, and the wounds had almost completely closed by Day 10. Therefore, the proposed hydrogel material can accelerate wound repair through multiple processes, showing tremendous clinical application potential for treating infected wounds.

Author Contributions W.D.: methodology, investigation, supervision, funding acquisition and writing-draft. H.L.: methodology, investigation, data curation, and writing-draft preparation. J.L.: methodology and investigation. Y.W.: methodology and investigation. Q.X.: investigation and data curation. J.L.: validation and methodology. S.Y.: funding acquisition, and supervision. J.L.: supervision, data curation, and editing. F.X.: conceptualization, funding acquisition, project administration, supervision, and validation. All authors reviewed the manuscript.

Funding This work was supported by the National Natural Science Foundation of China (21906077, 82073604), the Natural Science Foundation of Hunan Province (2020JJ5474), the Scientific Research Foundation of Hunan Provincial Education Department (23A0346), the Postdoctoral Science Foundation of China (2021M701161, 2021M690053), the Natural Science Foundation of Shandong Province (ZR2020QB095), and the Changsha Municipal Natural Science Foundation (kq2202144).

Data availability All data generated or analyzed during this study are included in this published article and its supplementary information files.

Declarations

Consent for publication All authors approved the final version of the manuscript.

Ethical approval The animal studies were performed in accordance with the U.K. Animals (Scientific Procedures) Act, 1986 and associated guidelines, EU Directive 2010/63/EU for animal experiments. This study was approved by the ethics committee of University of the South China and was performed in accordance with the university guidelines.

Competing interest The authors declare no competing interests.

References

Alzarea AI, Alruwaili NK, Ahmad MM, Munir MU, Butt AM, Alrowaili ZA, Shahari MSB, Almalki ZS, Alqahtani SS, Dolzhenko AV, Ahmad N (2022) Development and characterization of gentamicin-loaded arabinoxylan-sodium alginate films as antibacterial wound dressing. Int J Mol Sci 23(5):2899

Cao J, Hu S, Tang W, Wang Y, Yang Y, Wang F, Guo X, Ying Y, Liu X, Wen Y, Yang H (2023) Reactive hydrogel patch for SERS detection of environmental formaldehyde. ACS Sens 8(5):1929–1938

Chang G, Dang Q, Liu C, Wang X, Song H, Gao H, Sun H, Zhang B, Cha D (2022) Carboxymethyl chitosan and carboxymethyl cellulose based self-healing hydrogel for accelerating diabetic wound healing. Carbohydr Polym 292:119687

Chen K, Pan H, Ji D, Li Y, Duan H, Pan W (2021) Curcumin-loaded sandwich-like nanofibrous membrane prepared by electrospinning technology as wound dressing for accelerate wound healing. Mater Sci Eng C 127:112245

Cui H, Cui B, Chen H, Geng X, Geng X, Li Z, Cao S, Shen J, Li J (2023) A chitosan-based self-healing hydrogel for accelerating infected wound healing. Biomater Sci 11:4226–4237

Ding X, Li G, Zhang P, Jin E, Xiao C, Chen X (2021) Injectable self-healing hydrogel wound dressing with cysteine-specific on-demand dissolution property based on tandem dynamic covalent bonds. Adv Funct Mater 31(19):2011230

Dong H, Wang L, Du L, Wang X, Li Q, Wang X, Zhang J, Nie J, Ma G (2022) Smart polycationic hydrogel dressing for dynamic wound healing. Small 18(25):2201620

Dong Y, Li Y, Fan B, Peng W, Qian W, Ji X, Gan D, Liu P (2023) Long-term antibacterial, antioxidative, and bioadhesive hydrogel wound dressing for infected wound healing applications. Biomater Sci 11(6):2080–2090

Du S, Suo H, Xie G, Lyu Q, Mo M, Xie Z, Zhou N, Zhang L, Tao J, Zhu J (2022) Self-powered and photothermal electronic skin patches for accelerating wound healing. Nano Energy 93:106906

Du W, Liu J, Li H, Deng C, Luo J, Feng Q, Tan Y, Yang S, Wu Z, Xiao F (2023) Competition-based two-dimensional photonic crystal dually cross-linked supramolecular hydrogel for colorimetric and fluorescent dual-mode sensing of bisphenol A. Anal Chem 95(8):4220–4226

Guo B, Liang Y, Dong R (2023) Physical dynamic double-network hydrogels as dressings to facilitate tissue repair. Nat Protoc 18:3322–3354

Hu C, Long L, Cao J, Zhang S, Wang Y (2021) Dual-crosslinked mussel-inspired smart hydrogels with enhanced antibacterial and angiogenic properties for chronic infected diabetic wound treatment via pH-responsive quick cargo release. Chem Eng J 411:128564

Li J, Mooney DJ (2016) Designing hydrogels for controlled drug delivery. Nat Rev Mater 1:16071

Li Y, Yu P, Wen J, Sun H, Wang D, Liu J, Li J, Chu H (2022) Nanozyme-based stretchable hydrogel of low hysteresis with antibacterial and antioxidant dual functions for closely fitting and wound healing in movable parts. Adv Funct Mater 32(13):2110720

Liang Y, Li M, Yang Y, Qiao L, Xu H, Guo B (2022) pH/glucose dual responsive metformin release hydrogel dressings with adhesion and self-healing via dual-dynamic bonding for athletic diabetic foot wound healing. ACS Nano 16(2):3194–3207

Liu B, Li J, Zhang Z, Roland JD, Lee BP (2022) pH responsive antibacterial hydrogel utilizing catechol–boronate complexation chemistry. Chem Eng J 441:135808

Mallakpour S, Tukhani M, Hussain CM (2021) Recent advancements in 3D bioprinting technology of carboxymethyl cellulose-based hydrogels: Utilization in tissue engineering. Adv Colloid Interface Sci 292:102415

Patil P, Russo KA, McCune JT et al (2022) Reactive oxygen species–degradable polythioketal urethane foam dressings to promote porcine skin wound repair. Sci Transl Med 14(641):6586

Qian Y, Zheng Y, Jin J, Wu X, Xu K, Dai M, Niu Q, Zheng H, He X, Shen J (2022) Immunoregulation in diabetic wound repair with a photoenhanced glycyrrhizic acid hydrogel scaffold. Adv Mater 34(29):2200521

Qiao L, Liang Y, Chen J, Huang Y, Alsareii SA, Alamri AM, Harraz FA, Guo B (2023) Antibacterial conductive self-healing hydrogel wound dressing with dual dynamic bonds promotes infected wound healing. Bioact Mater 30:129–141

Qu F, Geng R, Liu Y, Zhu J (2022) Advanced nanocarrier-and microneedle-based transdermal drug delivery strategies for skin diseases treatment. Theranostics 12(7):3372–3406

Ran P, Zheng H, Cao W, Jia X, Zhang G, Liu Y, Li X (2022) On-demand changeable theranostic hydrogels and visual imaging-guided antibacterial photodynamic therapy to promote wound healing. ACS Appl Mater Interfaces 14(43):49375–49388

Sharma AK, Priya KBS, Shree B, Simran S (2021) Borax mediated synthesis of a biocompatible self-healing hydrogel using dialdehyde carboxymethyl cellulose-dextrin and gelatin. React Funct Polym 166:104977

Shen Y, Wang Z, Wang Y, Meng Z, Zhao Z (2021) A self-healing carboxymethyl chitosan/oxidized carboxymethyl cellulose hydrogel with fluorescent bioprobes for glucose detection. Carbohydr Polym 274:118642

Sun L, Fan L, Bian F, Chen G, Wang Y, Zhao Y (2021) MXene-integrated microneedle patches with innate molecule encapsulation for wound healing. Research 2021:9838490

Sun L, Wang Y, Fan L, Zhao Y (2023) Multifunctional microneedle patches with aligned carbon nanotube sheet basement for promoting wound healing. Chem Eng J 457:141206

Tang Z, Zhang Y, Zhang S, Gao Y, Duan Y, Zeng T, Zhou S (2022a) Temporal dynamics of antibiotic resistant bacteria and antibiotic resistance genes in activated sludge upon exposure to starvation. Sci Total Environ 840:156594

Tang Z, Zhang Y, Xiao S, Gao Y, Duan Y, Liu B, Xiong C, Yang Z, Wu Y, Zhou S (2022b) Insight into the impacts and mechanisms of ketone stress on the antibiotic resistance in Escherichia coli. Environ Sci Pollut Res 29:83746–83755

Tang W, Gu Z, Chu Y, Lv J, Fan L, Wang F, Ying Y, Zhang J, Jiang Y, Cao J, Zhu A, Yang H (2023) Magnetically-oriented porous hydrogel advances wearable electrochemical solidoid sensing heavy metallic ions. Chem Eng J 453:139902

Wang Y, Xiao G, Peng Y, Chen L, Fu S (2019) Effects of cellulose nanofibrils on dialdehyde carboxymethyl cellulose based dual responsive self-healing hydrogel. Cellulose 26:8813–8827

Wang J, Cheng H, Chen W, Han P, Yao X, Tang B, Duan W, Li P, Wei X, Chu PK, Zhang X (2023) An injectable, self-healing composite hydrogel with enhanced near-infrared photo-antibacterial therapeutic effects for accelerated wound healing. Chem Eng J 452:139474

Weinstein L (1985) Gram-negative bacterial infections: a look at the past, a view of the present, and a glance at the future. Rev Infect Dis 7:S538–S544

Xiao F, Li G, Wu Y, Chen Q, Wu Z, Yu R (2016) Label-free photonic crystal-based β-lactamase biosensor for β-lactam antibiotic and β-lactamase inhibitor. Anal Chem 88(18):9207–9212

Xiao F, Sun Y, Du W, Shi W, Wu Y, Liao S, Wu Z, Yu R (2017) Smart photonic crystal hydrogel material for uranyl ion monitoring and removal in water. Adv Funct Mater 27(42):1702147

Xiao F, Li H, Xie P, Liu J, Du W, Li L, Yang S, Wu Z (2022) Colloidal templating of highly ordered porous amidoxime-functionalized hydrogel for intelligent treatment of uranium contaminated water. Chem Eng J 431:134141

Xie F, Zou L, Xu Z, Ou X, Guo W, Gao Y, Gao G (2022) Alginate foam gel modified by graphene oxide for wound dressing. Int J Biol Macromol 223:391–403

Yang C, Ding X, Yang C, Shang L, Zhao Y (2023) Marine polymers-alginate/chitosan composited microcapsules for wound healing. Chem Eng J 456:140886

Yue Y, Gong X, Jiao W, Li Y, Yin X, Si Y, Yu J, Ding B (2021) In-situ electrospinning of thymol-loaded polyurethane fibrous membranes for waterproof, breathable, and antibacterial wound dressing application. J Colloid Interface Sci 592:310–318

Zhang YS, Khademhosseini A (2017) Advances in engineering hydrogels. Science 356(6337):eaaf3627

Zhang M, Yang M, Woo MW, Li Y, Han W, Dang X (2021) High-mechanical strength carboxymethyl chitosan-based hydrogel film for antibacterial wound dressing. Carbohydr Polym 256:117590

Zhao X, Liang Y, Huang Y, He J, Han Y, Guo B (2020) Physical double-network hydrogel adhesives with rapid shape adaptability, fast self-healing, antioxidant and NIR/pH stimulus-responsiveness for multidrug-resistant bacterial infection and removable wound dressing. Adv Funct Mater 30(17):1910748

Zhao Y, Huang L, Lin G, Tong M, Xie Y, Pan H, Shangguan J, Yao Q, Xu S, Xu H (2022) Skin-adaptive film dressing with smart-release of growth factors accelerated diabetic wound healing. Int J Biol Macromol 222:2729–2743

Zhou S, Yang Z, Zhang S, Gao Y, Tang Z, Duan Y, Zhang Y, Wang Y (2023) Metagenomic insights into the distribution, mobility, and hosts of extracellular antibiotic resistance genes in activated sludge under starvation stress. Water Res 236:119953

Zhu X, Liu L, Cao W, Yuan R, Wang H (2023) Ultra-sensitive microRNA biosensor based on strong aggregation-induced electrochemiluminescence from bidentate ligand-stabilized copper nanoclusters in polymer hydrogel. Anal Chem 95(13):5553–5560

Zou CY, Lei XX, Hu JJ, Jiang YL, Li QJ, Song YT, Zhang QY, Li-Ling J, Xie HQ (2022) Multi-crosslinking hydrogels with robust bio-adhesion and pro-coagulant activity for first-aid hemostasis and infected wound healing. Bioact Mater 16:388–402